Strong Gravitational Lensing in the Era of Big Data
Proceedings IAU Symposium No. 381, 2024
H. Stacey, A. Sonnenfeld & C. Grillo, eds.
doi:10.1017/S174392132300368X

Where are the Eddington-limited starbursts? Gravitational lensing provides a way forward for sub-kiloparsec views of star formation

Patrick S. Kamieneski

Arizona State University
email: pkamiene@asu.edu

Abstract. In the past decade, submillimeter surveys have been employed to define samples of gravitationally-lensed dusty star-forming galaxies (DSFGs) at $z \sim 1-4$. These extreme objects ($L_{\rm IR} = 10^{12} - 10^{13.5}$ $L_\odot$) appear to form stars prodigiously at rates of $100 - 3000$ $M_\odot$ yr^{-1}. Using all-sky *Planck* and *WISE* surveys, and wide-area *Herschel* surveys, we have identified the PASSAGES sample, with some of the rarest hyper-luminous IR galaxies ever discovered. We have found that their globally-averaged star formation surface densities are always sub-Eddington, typically by an order of magnitude. This may suggest that our understanding of how radiation pressure from massive stars disrupts the collapse of molecular clouds (thereby quenching star formation) is flawed—or simply that smaller physical resolutions are necessary. With the aid of lensing, we can now capture the source-plane distribution of star formation at $\sim$100pc scales, letting us identify isolated super-Eddington regions where quenching is occurring.

Keywords. Strong gravitational lensing (1643), Starburst galaxies (1570), Ultraluminous infrared galaxies (1735)

1. Introduction

Stellar feedback—the deposition of momentum and energy into the interstellar medium (ISM) by the formation of stars—has come to be accepted as a fundamental process governing the evolution of a galaxy. In particular, this feedback appears to be responsible for preventing gas-rich galaxies from rapidly converting gas into stars at a rate consistent with the free-fall time (see review McKee and Ostriker 2007). This feedback has impacts on global scales of a galaxy, but is ultimately a more local process. The efficiency of star formation is low on galaxy-wide scales; defined as $\varepsilon_{\rm ff} \equiv \tau_{\rm ff} \cdot {\rm SFR}/M_{\rm gas}$—with star-formation rate SFR, total gas mass $M_{\rm gas}$, and free-fall time $\tau_{\rm ff}$—typical values are of order 1% (e.g. Kennicutt 1998; Krumholz and McKee 2005; Krumholz et al. 2012; Padoan and Nordlund 2011; Federrath and Klessen 2012; Utomo et al. 2018). Yet, the efficiency for giant molecular clouds (GMCs) themselves can be much higher, even approaching unity in some instances (e.g., Murray 2011). These observational constraints to test models of star formation have been difficult to derive, so it remains unclear what physical processes dominate in regulating the collapse of molecular gas.

Scoville (2003), Murray et al. (2005), and Thompson et al. (2005) first developed theoretical models by which radiation pressure in dusty environments could become the predominant source of stellar feedback. In particular, where the ISM is optically thick to IR emission (resulting from the reprocessing of UV photons from massive stars), the momentum of the photons against dust grains coupled to the gas becomes an efficient support against the self-gravity of molecular clouds. Such an environment

is expected for objects like ultra-luminous infrared galaxies (ULIRGs; Lonsdale et al. 2006)—or more generally the population of dusty star-forming galaxies (DSFGs)—which host extreme dust-enshrouded starbursts. This Eddington-like limit at which radiation pressure exceeds self-gravity is estimated to occur at star formation rate surface densities of around $\Sigma_{\rm SFR} \equiv {\rm SFR}/(2\pi R_{\rm eff}^2) \sim 1000\ M_\odot\ {\rm yr}^{-1}\ {\rm kpc}^{-2}$ (Andrews and Thompson 2011; Simpson et al. 2015). However, as this limit is for globally-averaged $\Sigma_{\rm SFR}$, galaxies forming stars at overall sub-Eddington densities can still host super-Eddington clumps of star formation. Moreover, the measurement of effective radii $R_{\rm eff}$ for high-z (often compact) galaxies requires finer angular resolution than local ULIRGs. For these reasons, the application of gravitational lensing as a "cosmic telescope" is required to make progress in testing models of stellar feedback.

2. Sample Definition and Data

For this analysis, we employ the lensed DSFGs selected with *Planck* as part of the PASSAGES sample (*Planck* All-Sky Survey to Analyze Gravitationally-lensed Extreme Starbursts; Harrington et al. 2016, 2021; Berman et al. 2022; lens models from Kamieneski et al. 2023). We also make some comparisons to similar samples defined with the South Pole Telescope (SPT; e.g., Weiss et al. 2013; lens models from Spilker et al. 2016) and *Herschel* (e.g., Negrello et al. 2010, 2017; Wardlow et al. 2013; lens models from Bussmann et al. 2013, 2015). As the *Planck*-selected objects occupy the upper echelon of apparent infrared luminosities for their redshift range of $z \sim 1-3.5$ (see also objects identified independently by Cañameras et al. 2015), they offer perhaps the ideal view of extreme starburst events. Moreover, radiative transfer modeling of multi-transition molecular gas lines for the PASSAGES sample by Harrington et al. (2021) suggested that some objects would approach this limit, based on the ratio of their $L_{\rm IR}$ to ISM mass (relative to the threshold of 500 $L_\odot/M_\odot$; see Scoville 2003). Since the total flux-weighted magnifications for extended objects (i.e., starbursts rather than quasars) generally tend not to exceed $\mu \sim 10-20$ (e.g., Hezaveh et al. 2012), their large apparent luminosities were perhaps more easily explained by larger intrinsic luminosities rather than larger magnifications. As such, they are among the best candidates for maximal starbursts forming stars at surface densities close to (or above) the Eddington limit.

Apparent star formation rates were derived from their total infrared luminosities (Harrington et al. 2016; Berman et al. 2022), which captures the UV emission from massive stars that is reprocessed into the IR by dust. As this covers a wide wavelength regime, for which the spatial distribution of continuum can vary, it is not entirely trivial to characterize the size of the dust-emitting region. For our purpose, we use 1.1mm continuum imaging (rest-frame $\sim 250-500\mu$m) on the Rayleigh-Jeans tail. Band 6 ($1.1-1.4$ mm) observations were taken with the Atacama Large Millimeter/submillimeter Array as part of Cycle 5 program 2017.1.01214.S (PI: M. Yun), reaching synthesized beam resolutions of $0.4-0.8''$ and sensitivities of $0.07-0.33$ mJy. The PASSAGES sub-sample that has been observed with ALMA and has a credible strong lens model consists of 13 objects. Further details on the observations are provided in Berman et al. (2022) and Kamieneski et al. (2023).

3. Results and Discussion

Fortunately, the measurement of $\Sigma_{\rm SFR}$ is relatively insensitive to statistical and systematic uncertainties in the lens model, as it is connected to surface brightness, which is conserved by gravitational lensing. For example, if a lens model erroneously overestimates a galaxy size by a factor of k relative to the "true" value, then the magnification measured from the ratio of image-plane to source-plane area will be underestimated by

https://doi.org/10.1017/S174392132300368X Published online by Cambridge University Press

a factor of $\sim k^2$; this then leads to factor of k^2 overestimate of the intrinsic luminosity $L_{\rm IR}$. As a result of this, both the numerator and denominator of $\Sigma_{\rm IR} = L_{\rm IR}/(2\pi R_{\rm eff}^2)$ are overestimated by k^2, and the effect essentially cancels out. Considered slightly differently, $\Sigma_{\rm IR}$ and $\Sigma_{\rm SFR}$ could even be measured directly from the image-plane, lensing-uncorrected data, were it not for the challenge that shear distorts the shape of the galaxy and makes the determination of effective radius more complicated. As a more direct comparison with unlensed DSFGs is desirable, we carry out lens modeling in order to estimate the global surface densities of star formation.

Full details of our lens modeling approach for the PASSAGES sample are presented in Kamieneski et al. (2023), but we summarize it in brief here. Only the foreground lensing mass is parameterized (typically with singular isothermal ellipsoid profiles, Kormann et al. 1994), with constraints set by only the locations of multiply-imaged components. These image families are determined using multi-wavelength information from *Hubble* Space Telescope (HST) at 1.6 μm, Gemini-S Observatory at r' and z' bands, ALMA at 1.1mm, and the *Karl G. Jansky* Very Large Array at 6 GHz. Models are optimized through Markov Chain Monte Carlo with LENSTOOL (Kneib et al. 1996; Jullo et al. 2007; Jullo and Kneib 2009), effectively minimizing the RMS of image-plane separations between observed vs. predicted image locations. Magnifications (and associated uncertainties) are estimated by randomly sampling from the multi-dimensional posterior distribution, reconstructing in the source plane by ray-tracing, and computing the ratio of image-plane to source-plane areas. Objects are reconstructed in the source plane without parameterization or regularization, as these extreme starbursts may be clumpy and highly irregular. A similar approach is taken for measuring intrinsic effective radii and uncertainties (see also Section 3 of Kamieneski et al. 2023).

Figure 1 shows the globally-averaged $\Sigma_{\rm SFR}$ vs. $R_{\rm eff}$ of the dust continuum for three samples of lensed DSFGs, with intrinsic values derived with lens models: PASSAGES (this work, and see Table 3 from Kamieneski et al. 2023), SPT (Spilker et al. 2016), and *Herschel* (Bussmann et al. 2013). Additionally, unlensed DSFGs from the ALESS sample with resolved size measurements from Hodge et al. (2019) are shown. We find that very few of the objects shown approach the theoretical Eddington limit (with none surpassing it), and the median value of the four samples ($\Sigma_{\rm SFR} \sim 58\ M_\odot\ {\rm yr}^{-1}\ {\rm kpc}^{-2}$, $R_{\rm eff} \sim 1.6$ kpc) is more than an order of magnitude below the threshold. This is in apparent contrast to local ultra-luminous infrared galaxies (ULIRGs; $L_{\rm IR} = 10^{12-13}\ L_\odot$), which have been found to frequently exceed the Eddington limit, even by over an order of magnitude in some cases (e.g., Barcos-Muñoz et al. 2017; Pereira-Santaella et al. 2021). The canonical and well-studied ULIRG Arp 220, for example, has regions forming stars at surface densities of $\Sigma_{\rm SFR} \sim 10^{4.1\pm0.1}\ M_\odot\ {\rm yr}^{-1}\ {\rm kpc}^{-2}$ (Barcos-Muñoz et al. 2015). On the other hand, Song et al. (2022) found predominantly sub-Eddington star formation in a broader sample of local luminous infrared galaxies (LIRGs; $L_{\rm IR} = 10^{11-12}\ L_\odot$) and ULIRGs. If the extreme hyper-luminous IR galaxies (HyLIRGs; $L_{\rm IR} > 10^{13}\ L_\odot$) seen at high-$z$ like the PASSAGES objects are in fact sub-Eddington, it might suggest simply that their order-of-magnitude increase in IR luminosity over ULIRGs is accompanied by a comparable ~ 0.5 dex increase in radius. Indeed, for a very large sample of 1000+ DSFGs covering LIRGs, ULIRGs, and a handful of HyLIRGs from $z = 0 - 6$, Fujimoto et al. (2017) found a highly significant correlation between $R_{\rm eff}$ and $L_{\rm IR}$, fit approximately by $R_{\rm eff} \propto L_{\rm IR}^{0.28\pm0.07}$ (albeit with large scatter). The authors speculate that the power-law slope could be set by processes of disk formation, given the similarity in slope for UV-detected star-forming galaxies (e.g., $\alpha_{\rm UV} = 0.27 \pm 0.01$, Shibuya et al. 2015). While perhaps a too simplistic picture for complicated high-z systems, it is useful to consider that the Stefan-Boltzmann law suggests that an optically-thick spherical blackbody should radiate as $L_{\rm IR} \propto R_{\rm eff}^2 T_{\rm dust}^4$.

https://doi.org/10.1017/S174392132300368X Published online by Cambridge University Press

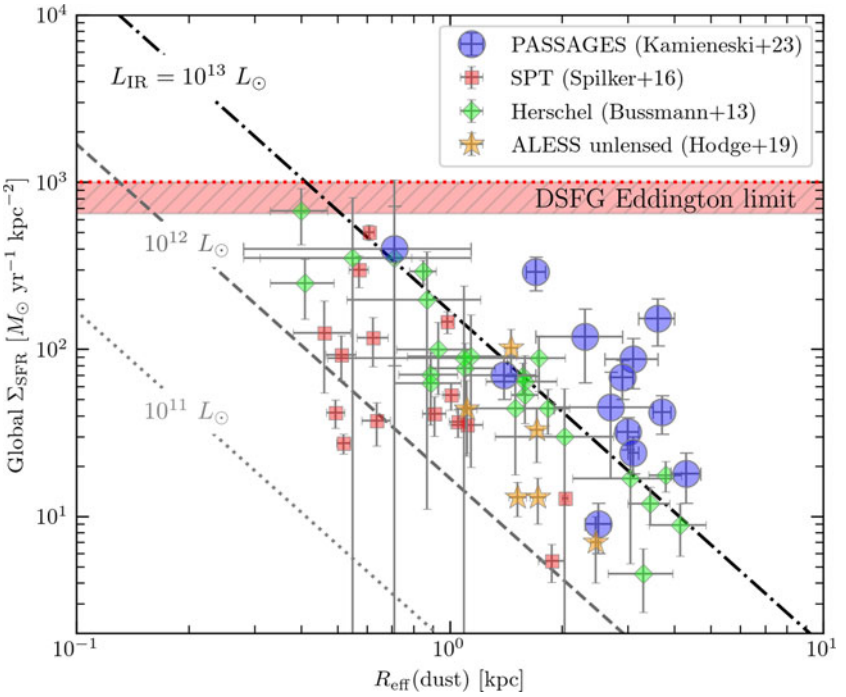

Figure 1. The galaxy-averaged star formation rate surface density $\Sigma_{\rm SFR}$ vs. dust continuum effective radius $R_{\rm eff}$ for members of the PASSAGES sample (Kamieneski et al. 2023), as measured in the model-reconstructed source plane. Also shown are the source-plane values for samples of lensed DSFGs identified with SPT (Spilker et al. 2016) and *Herschel* (Bussmann et al. 2013), alongside unlensed DSFGs from the ALESS sample (Hodge et al. 2019). The Eddington limit is typically computed at values of $\Sigma_{\rm SFR} \sim 650 - 1000\ M_\odot\ {\rm yr}^{-1}\ {\rm kpc}^{-2}$ (depending on choice of gas mass fraction and dust-to-gas ratio; Andrews and Thompson 2011; Simpson et al. 2015; Hodge et al. 2019), which is shown as a red shaded region. Diagonal dotted, dashed, and dash-dotted lines indicate the loci for IR luminosities of $10^{11}\ L_\odot$ (LIRGs), $10^{12}\ L_\odot$ (ULIRGs), and $10^{13}\ L_\odot$ (hyper-luminous infrared galaxies or HyLIRGs).

However, as noted by Simpson et al. (2015), "clumpy" distributions of star formation with isolated sub-galactic regions—e.g., star-forming complexes and individual GMCs—forming stars above the Eddington limit could still appear sub-Eddington in its galaxy-wide star formation rate surface density. For this reason, in future work, we intend to directly map $\Sigma_{\rm SFR}$ at $\sim 100 - 500$pc scales with newly-obtained $\theta \sim 0.1''$ resolution ALMA observations of 16 PASSAGES objects at 870μm and 1.1mm. Even with very high-resolution $\theta \sim 0.07''$ ALMA imaging of six ALESS DSFGs, reaching 500pc physical scales, Hodge et al. (2019) found that both the peak and the globally-averaged $\Sigma_{\rm SFR}$ values remained sub-Eddington. However, these values were actually consistent with those of local ULIRGs from Barcos-Muñoz et al. (2017) with comparable physical sizes, and only ULIRGs with smaller effective radii ($\lesssim 0.2$ kpc) were found to be super-Eddington. Hodge et al. suggested this as a sign that even smaller physical scales need to be probed to find super-Eddington star formation in the distant Universe. Indeed, reaching physical scales of $\sim 60 - 160$ pc with lensing, Cañameras et al. (2017) found local densities of $\sim 1000 - 2000\ M_\odot\ {\rm yr}^{-1}\ {\rm kpc}^{-2}$. At present, these resolutions are only feasibly accessible with the longest-baseline configurations of facilities like ALMA, and with the aid of gravitational lensing. However, the move to 100 pc scales also brings additional challenges. For example, measurement of the properties of small star-forming clumps may be more

https://doi.org/10.1017/S174392132300368X Published online by Cambridge University Press

affected by gravitational microlensing (e.g., Fian et al. 2021), or by millilensing from dark, low-mass substructures in the lensing galaxy or anywhere along the line-of-sight (e.g., Mao and Schneider 1998; Vegetti et al. 2012, 2014; Inoue 2016; Nierenberg et al. 2017, 2020). Such effects are negligible at coarser resolutions, but they should be incorporated into uncertainties when approaching GMC scales. Fortunately, the conservation of surface brightness from lensing may again work to our advantage when mapping $\Sigma_{\rm SFR}$, whereas the measurement of absolute properties like the mass and luminosity of clumps is made more difficult.

Finally, we consider the future of submillimeter-selected samples of gravitational lenses like PASSAGES, which offer valuable laboratories for examining extreme star formation at ultra-high resolutions. At present, the PASSAGES sample consists of $\sim$30 lensed DSFGs (Harrington et al. 2016; Berman et al. 2022). Other samples from *Planck*—and from facilities like *Herschel*, SPT, Atacama Cosmology Telescope (ACT)—contain an additional several hundred such lenses (e.g., Negrello et al. 2010, 2017; Vieira et al. 2010; González-Nuevo et al. 2012; Wardlow et al. 2013; Weiss et al. 2013; Su et al. 2017; Bakx et al. 2020a,b; Gralla et al. 2020; Trombetti et al. 2021; Lammers et al. 2022). While predicted by Blain (1996) and Negrello et al. (2007), submillimeter flux selection of gravitational lenses has proven to be remarkably efficacious, with few contaminants.

Novel selection criteria and new facilities will continue to increase this sample of lensed submillimeter-bright objects in the coming decade. As one notable example, the TolTEC camera of the Large Millimeter Telescope will have unprecedented sensitive mapping capabilities at 1.1mm, 1.4mm, and 2.1mm simultaneously (Wilson et al. 2020). This longer-wavelength regime could particularly help in accessing higher-redshift ($z \gtrsim 4$) lensed DSFGs (see, e.g., Casey et al. 2021). With this growing sample of lensed, intrinsically extreme starbursts—alongside the anticipated large ensemble of more than 10^5 optically-selected lenses with new mapping facilities like *Euclid* (e.g. Laureijs et al. 2011; Serjeant 2014)—new frontiers are being opened up for testing theoretical frameworks for star formation and the dynamics of the interstellar medium. Strong gravitational lensing will continue to be a crucial tool in helping to bridge the gap in the physical resolutions that we can reach for the local vs. high-redshift Universe.

References

Andrews, B. H. & Thompson, T. A. 2011, Assessing Radiation Pressure as a Feedback Mechanism in Star-forming Galaxies. *ApJ*, 727(2), 97.

Bakx, T. J. L. C., Dannerbauer, H., Frayer, D., Eales, S. A., Pérez-Fournon, I., Cai, Z. Y., Clements, D. L., De Zotti, G., González-Nuevo, J., Ivison, R. J., Lapi, A., Michałowski, M. J., Negrello, M., Serjeant, S., Smith, M. W. L., Temi, P., Urquhart, S., & van der Werf, P. 2020,a IRAM 30-m-EMIR redshift search of z = 3-4 lensed dusty starbursts selected from the HerBS sample. *MNRAS*, 496a(2), 2372–2390.

Bakx, T. J. L. C., Eales, S., & Amvrosiadis, A. 2020,b A search for the lenses in the Herschel Bright Sources (HerBS) sample. *MNRAS*, 493b(3), 4276–4293.

Barcos-Muñoz, L., Leroy, A. K., Evans, A. S., Condon, J., Privon, G. C., Thompson, T. A., Armus, L., Díaz-Santos, T., Mazzarella, J. M., Meier, D. S., Momjian, E., Murphy, E. J., Ott, J., Sanders, D. B., Schinnerer, E., Stierwalt, S., Surace, J. A., & Walter, F. 2017, A 33 GHz Survey of Local Major Mergers: Estimating the Sizes of the Energetically Dominant Regions from High-resolution Measurements of the Radio Continuum. *ApJ*, 843(2), 117.

Barcos-Muñoz, L., Leroy, A. K., Evans, A. S., Privon, G. C., Armus, L., Condon, J., Mazzarella, J. M., Meier, D. S., Momjian, E., Murphy, E. J., Ott, J., Reichardt, A., Sakamoto, K., Sanders, D. B., Schinnerer, E., Stierwalt, S., Surace, J. A., Thompson, T. A., & Walter, F. 2015, High-resolution Radio Continuum Measurements of the Nuclear Disks of Arp 220. *ApJ*, 799(1), 10.

https://doi.org/10.1017/S174392132300368X Published online by Cambridge University Press

Berman, D. A., Yun, M. S., Harrington, K. C., Kamieneski, P., Lowenthal, J., Frye, B. L., Wang, Q. D., Wilson, G. W., Aretxaga, I., Chavez, M., Cybulski, R., De la Luz, V., Erickson, N., Ferrusca, D., Hughes, D. H., Montaña, A., Narayanan, G., Sánchez-Argüelles, D., Schloerb, F. P., Souccar, K., Terlevich, E., Terlevich, R., & Zavala, J. A. 2022, PASSAGES: the Large Millimeter Telescope and ALMA observations of extremely luminous high-redshift galaxies identified by the Planck. *MNRAS*, 515(3), 3911–3937.

Blain, A. W. 1996, Galaxy-galaxy gravitational lensing in the millimetre/submillimetre waveband. *MNRAS*, 283, 1340–1348.

Bussmann, R. S., Pérez-Fournon, I., Amber, S., Calanog, J., Gurwell, M. A., Dannerbauer, H., De Bernardis, F., Fu, H., Harris, A. I., Krips, M., Lapi, A., Maiolino, R., Omont, A., Riechers, D., Wardlow, J., Baker, A. J., Birkinshaw, M., Bock, J., Bourne, N., Clements, D. L., Cooray, A., De Zotti, G., Dunne, L., Dye, S., Eales, S., Farrah, D., Gavazzi, R., González Nuevo, J., Hopwood, R., Ibar, E., Ivison, R. J., Laporte, N., Maddox, S., Martínez-Navajas, P., Michalowski, M., Negrello, M., Oliver, S. J., Roseboom, I. G., Scott, D., Serjeant, S., Smith, A. J., Smith, M., Streblyanska, A., Valiante, E., van der Werf, P., Verma, A., Vieira, J. D., Wang, L., & Wilner, D. 2013, Gravitational Lens Models Based on Submillimeter Array Imaging of Herschel-selected Strongly Lensed Sub-millimeter Galaxies at z $>$ 1.5. *ApJ*, 779, 25.

Bussmann, R. S., Riechers, D., Fialkov, A., Scudder, J., Hayward, C. C., Cowley, W. I., Bock, J., Calanog, J., Chapman, S. C., Cooray, A., De Bernardis, F., Farrah, D., Fu, H., Gavazzi, R., Hopwood, R., Ivison, R. J., Jarvis, M., Lacey, C., Loeb, A., Oliver, S. J., Pérez-Fournon, I., Rigopoulou, D., Roseboom, I. G., Scott, D., Smith, A. J., Vieira, J. D., Wang, L., & Wardlow, J. 2015, HerMES: ALMA Imaging of Herschel-selected Dusty Star-forming Galaxies. *ApJ*, 812, 43.

Cañameras, R., Nesvadba, N., Kneissl, R., Frye, B., Gavazzi, R., Koenig, S., Le Floc'h, E., Limousin, M., Oteo, I., & Scott, D. 2017, Planck's dusty GEMS. IV. Star formation and feedback in a maximum starburst at z = 3 seen at 60-pc resolution. *A&A*, 604, A117.

Cañameras, R., Nesvadba, N. P. H., Guery, D., McKenzie, T., König, S., Petitpas, G., Dole, H., Frye, B., Flores-Cacho, I., Montier, L., Negrello, M., Beelen, A., Boone, F., Dicken, D., Lagache, G., Le Floc'h, E., Altieri, B., Béthermin, M., Chary, R., de Zotti, G., Giard, M., Kneissl, R., Krips, M., Malhotra, S., Martinache, C., Omont, A., Pointecouteau, E., Puget, J.-L., Scott, D., Soucail, G., Valtchanov, I., Welikala, N., & Yan, L. 2015, Planck's dusty GEMS: The brightest gravitationally lensed galaxies discovered with the Planck all-sky survey. *A&A*, 581, A105.

Casey, C. M., Zavala, J. A., Manning, S. M., Aravena, M., Béthermin, M., Caputi, K. I., Champagne, J. B., Clements, D. L., Drew, P., Finkelstein, S. L., Fujimoto, S., Hayward, C. C., Dekel, A. M., Kokorev, V., Lagos, C. d. P., Long, A. S., Magdis, G. E., Man, A. W. S., Mitsuhashi, I., Popping, G., Spilker, J., Staguhn, J., Talia, M., Toft, S., Treister, E., Weaver, J. R., & Yun, M. 2021, Mapping Obscuration to Reionization with ALMA (MORA): 2 mm Efficiently Selects the Highest-redshift Obscured Galaxies. *ApJ*, 923(2), 215.

Federrath, C. & Klessen, R. S. 2012, The Star Formation Rate of Turbulent Magnetized Clouds: Comparing Theory, Simulations, and Observations. *ApJ*, 761(2), 156.

Fian, C., Mediavilla, E., Jiménez-Vicente, J., Motta, V., Muñoz, J. A., Chelouche, D., Goméz-Alvarez, P., Rojas, K., & Hanslmeier, A. 2021, Revealing the structure of the lensed quasar Q 0957+561. I. Accretion disk size. *A&A*, 654, A70.

Fujimoto, S., Ouchi, M., Shibuya, T., & Nagai, H. 2017, Demonstrating a New Census of Infrared Galaxies with ALMA (DANCING-ALMA). I. FIR Size and Luminosity Relation at z = 0-6 Revealed with 1034 ALMA Sources. *ApJ*, 850, 83.

González-Nuevo, J., Lapi, A., Fleuren, S., Bressan, S., Danese, L., De Zotti, G., Negrello, M., Cai, Z. Y., Fan, L., Sutherland, W., Baes, M., Baker, A. J., Clements, D. L., Cooray, A., Dannerbauer, H., Dunne, L., Dye, S., Eales, S., Frayer, D. T., Harris, A. I., Ivison, R., Jarvis, M. J., Michałowski, M. J., López-Caniego, M., Rodighiero, G., Rowlands, K., Serjeant, S., Scott, D., van der Werf, P., Auld, R., Buttiglione, S., Cava, A., Dariush, A.,

Fritz, J., Hopwood, R., Ibar, E., Maddox, S., Pascale, E., Pohlen, M., Rigby, E., Smith, D., & Temi, P. 2012, Herschel-ATLAS: Toward a Sample of ~1000 Strongly Lensed Galaxies. *ApJ*, 749(1), 65.

Gralla, M. B., Marriage, T. A., Addison, G., Baker, A. J., Bond, J. R., Crichton, D., Datta, R., Devlin, M. J., Dunkley, J., Dünner, R., Fowler, J., Gallardo, P. A., Hall, K., Halpern, M., Hasselfield, M., Hilton, M., Hincks, A. D., Huffenberger, K. M., Hughes, J. P., Kosowsky, A., López-Caraballo, C. H., Louis, T., Marsden, D., Moodley, K., Niemack, M. D., Page, L. A., Partridge, B., Rivera, J., Sievers, J. L., Staggs, S., Su, T., Swetz, D., & Wollack, E. J. 2020, Atacama Cosmology Telescope: Dusty Star-forming Galaxies and Active Galactic Nuclei in the Equatorial Survey. *ApJ*, 893(2), 104.

Harrington, K. C., Weiss, A., Yun, M. S., Magnelli, B., Sharon, C. E., Leung, T. K. D., Vishwas, A., Wang, Q. D., Frayer, D. T., Jiménez-Andrade, E. F., Liu, D., García, P., Romano-Díaz, E., Frye, B. L., Jarugula, S., Bădescu, T., Berman, D., Dannerbauer, H., Díaz-Sánchez, A., Grassitelli, L., Kamieneski, P., Kim, W. J., Kirkpatrick, A., Lowenthal, J. D., Messias, H., Puschnig, J., Stacey, G. J., Torne, P., & Bertoldi, F. 2021, Turbulent Gas in Lensed Planck-selected Starbursts at z $\sim$ 1-3.5. *ApJ*, 908(1), 95.

Harrington, K. C., Yun, M. S., Cybulski, R., Wilson, G. W., Aretxaga, I., Chavez, M., De la Luz, V., Erickson, N., Ferrusca, D., Gallup, A. D., Hughes, D. H., Montaña, A., Narayanan, G., Sánchez-Argüelles, D., Schloerb, F. P., Souccar, K., Terlevich, E., Terlevich, R., Zeballos, M., & Zavala, J. A. 2016, Early science with the Large Millimeter Telescope: observations of extremely luminous high-z sources identified by Planck. *MNRAS*, 458, 4383–4399.

Hezaveh, Y. D., Marrone, D. P., & Holder, G. P. 2012, Size Bias and Differential Lensing of Strongly Lensed, Dusty Galaxies Identified in Wide-Field Surveys. *ApJ*, 761, 20.

Hodge, J. A., Smail, I., Walter, F., da Cunha, E., Swinbank, A. M., Rybak, M., Venemans, B., Brandt, W. N., Calistro Rivera, G., Chapman, S. C., Chen, C.-C., Cox, P., Dannerbauer, H., Decarli, R., Greve, T. R., Knudsen, K. K., Menten, K. M., Schinnerer, E., Simpson, J. M., van der Werf, P., Wardlow, J. L., & Weiss, A. 2019, ALMA Reveals Potential Evidence for Spiral Arms, Bars, and Rings in High-redshift Submillimeter Galaxies. *ApJ*, 876, 130.

Inoue, K. T. 2016, On the origin of the flux ratio anomaly in quadruple lens systems. *MNRAS*, 461(1), 164–175.

Jullo, E. & Kneib, J.-P. 2009, Multiscale cluster lens mass mapping - I. Strong lensing modelling. *MNRAS*, 395, 1319–1332.

Jullo, E., Kneib, J.-P., Limousin, M., Elíasdóttir, Á., Marshall, P. J., & Verdugo, T. 2007, A Bayesian approach to strong lensing modelling of galaxy clusters. *New Journal of Physics*, 9, 447.

Kamieneski, P. S., Yun, M. S., Harrington, K. C., Lowenthal, J. D., Wang, Q. D., Frye, B. L., Jimenez-Andrade, E. F., Vishwas, A., Cooper, O., Pascale, M., Foo, N., Berman, D., Englert, A., & Garcia Diaz, C. 2023, PASSAGES: the wide-ranging, extreme intrinsic properties of Planck-selected, lensed dusty star-forming galaxies. *arXiv e-prints*, arXiv:2301.09746.

Kennicutt, Robert C., J. 1998, The Global Schmidt Law in Star-forming Galaxies. *ApJ*, 498(2), 541–552.

Kneib, J.-P., Ellis, R. S., Smail, I., Couch, W. J., & Sharples, R. M. 1996, Hubble Space Telescope Observations of the Lensing Cluster Abell 2218. *ApJ*, 471, 643.

Kormann, R., Schneider, P., & Bartelmann, M. 1994, Isothermal elliptical gravitational lens models. *A&A*, 284, 285–299.

Krumholz, M. R., Dekel, A., & McKee, C. F. 2012, A Universal, Local Star Formation Law in Galactic Clouds, nearby Galaxies, High-redshift Disks, and Starbursts. *ApJ*, 745(1), 69.

Krumholz, M. R. & McKee, C. F. 2005, A General Theory of Turbulence-regulated Star Formation, from Spirals to Ultraluminous Infrared Galaxies. *ApJ*, 630, 250–268.

Lammers, C., Hill, R., Lim, S., Scott, D., Cañameras, R., & Dole, H. 2022, Candidate high-redshift protoclusters and lensed galaxies in the Planck list of high-z sources overlapping with Herschel-SPIRE imaging. *MNRAS*, 514(4), 5004–5023.

Laureijs, R., Amiaux, J., Arduini, S., Augueres, J. L., Brinchmann, J., Cole, R., Cropper, M., Dabin, C., Duvet, L., Ealet, A., & et al. 2011, Euclid Definition Study Report. *arXiv e-prints*, arXiv:1110.3193.

Lonsdale, C. J., Farrah, D., & Smith, H. E. 2006, *Ultraluminous Infrared Galaxies*, 285. Springer-Verlag.

Mao, S. & Schneider, P. 1998, Evidence for substructure in lens galaxies? *MNRAS*, 295, 587.

McKee, C. F. & Ostriker, E. C. 2007, Theory of Star Formation. *ARA&A*, 45(1), 565–687.

Murray, N. 2011, Star Formation Efficiencies and Lifetimes of Giant Molecular Clouds in the Milky Way. *ApJ*, 729(2), 133.

Murray, N., Quataert, E., & Thompson, T. A. 2005, On the Maximum Luminosity of Galaxies and Their Central Black Holes: Feedback from Momentum-driven Winds. *ApJ*, 618(2), 569–585.

Negrello, M., Amber, S., Amvrosiadis, A., Cai, Z.-Y., Lapi, A., Gonzalez-Nuevo, J., De Zotti, G., Furlanetto, C., Maddox, S. J., Allen, M., Bakx, T., Bussmann, R. S., Cooray, A., Covone, G., Danese, L., Dannerbauer, H., Fu, H., Greenslade, J., Gurwell, M., Hopwood, R., Koopmans, L. V. E., Napolitano, N., Nayyeri, H., Omont, A., Petrillo, C. E., Riechers, D. A., Serjeant, S., Tortora, C., Valiante, E., Verdoes Kleijn, G., Vernardos, G., Wardlow, J. L., Baes, M., Baker, A. J., Bourne, N., Clements, D., Crawford, S. M., Dye, S., Dunne, L., Eales, S., Ivison, R. J., Marchetti, L., Michałowski, M. J., Smith, M. W. L., Vaccari, M., & van der Werf, P. 2017, The Herschel-ATLAS: a sample of 500 μm-selected lensed galaxies over 600 deg^2. *MNRAS*, 465, 3558–3580.

Negrello, M., Hopwood, R., De Zotti, G., Cooray, A., Verma, A., Bock, J., Frayer, D. T., Gurwell, M. A., Omont, A., Neri, R., Dannerbauer, H., Leeuw, L. L., Barton, E., Cooke, J., Kim, S., da Cunha, E., Rodighiero, G., Cox, P., Bonfield, D. G., Jarvis, M. J., Serjeant, S., Ivison, R. J., Dye, S., Aretxaga, I., Hughes, D. H., Ibar, E., Bertoldi, F., Valtchanov, I., Eales, S., Dunne, L., Driver, S. P., Auld, R., Buttiglione, S., Cava, A., Grady, C. A., Clements, D. L., Dariush, A., Fritz, J., Hill, D., Hornbeck, J. B., Kelvin, L., Lagache, G., Lopez-Caniego, M., Gonzalez-Nuevo, J., Maddox, S., Pascale, E., Pohlen, M., Rigby, E. E., Robotham, A., Simpson, C., Smith, D. J. B., Temi, P., Thompson, M. A., Woodgate, B. E., York, D. G., Aguirre, J. E., Beelen, A., Blain, A., Baker, A. J., Birkinshaw, M., Blundell, R., Bradford, C. M., Burgarella, D., Danese, L., Dunlop, J. S., Fleuren, S., Glenn, J., Harris, A. I., Kamenetzky, J., Lupu, R. E., Maddalena, R. J., Madore, B. F., Maloney, P. R., Matsuhara, H., Michałowski, M. J., Murphy, E. J., Naylor, B. J., Nguyen, H., Popescu, C., Rawlings, S., Rigopoulou, D., Scott, D., Scott, K. S., Seibert, M., Smail, I., Tuffs, R. J., Vieira, J. D., van der Werf, P. P., & Zmuidzinas, J. 2010, The Detection of a Population of Submillimeter-Bright, Strongly Lensed Galaxies. *Science*, 330, 800.

Negrello, M., Perrotta, F., González-Nuevo, J., Silva, L., de Zotti, G., Granato, G. L., Baccigalupi, C., & Danese, L. 2007, Astrophysical and cosmological information from large-scale submillimetre surveys of extragalactic sources. *MNRAS*, 377, 1557–1568.

Nierenberg, A. M., Gilman, D., Treu, T., Brammer, G., Birrer, S., Moustakas, L., Agnello, A., Anguita, T., Fassnacht, C. D., Motta, V., Peter, A. H. G., & Sluse, D. 2020, Double dark matter vision: twice the number of compact-source lenses with narrow-line lensing and the WFC3 grism. *MNRAS*, 492(4), 5314–5335.

Nierenberg, A. M., Treu, T., Brammer, G., Peter, A. H. G., Fassnacht, C. D., Keeton, C. R., Kochanek, C. S., Schmidt, K. B., Sluse, D., & Wright, S. A. 2017, Probing dark matter substructure in the gravitational lens HE 0435-1223 with the WFC3 grism. *MNRAS*, 471(2), 2224–2236.

Padoan, P. & Nordlund, Å. 2011, The Star Formation Rate of Supersonic Magnetohydrodynamic Turbulence. *ApJ*, 730(1), 40.

Pereira-Santaella, M., Colina, L., García-Burillo, S., Lamperti, I., González-Alfonso, E., Perna, M., Arribas, S., Alonso-Herrero, A., Aalto, S., Combes, F., Labiano, A., Piqueras-López, J., Rigopoulou, D., & van der Werf, P. 2021, Physics of ULIRGs with MUSE and ALMA: The PUMA project. II. Are local ULIRGs powered by AGN? The subkiloparsec view of the 220 GHz continuum. *A&A*, 651, A42.

Scoville, N. 2003, Starburst and AGN Connections and Models. *Journal of Korean Astronomical Society*, 36(3), 167–175.

Serjeant, S. 2014, Up to 100,000 Reliable Strong Gravitational Lenses in Future Dark Energy Experiments. *ApJL*, 793, L10.

Shibuya, T., Ouchi, M., & Harikane, Y. 2015, Morphologies of ∼190,000 Galaxies at z = 0-10 Revealed with HST Legacy Data. I. Size Evolution. *ApJS*, 219, 15.

Simpson, J. M., Smail, I., Swinbank, A. M., Almaini, O., Blain, A. W., Bremer, M. N., Chapman, S. C., Chen, C.-C., Conselice, C., Coppin, K. E. K., Danielson, A. L. R., Dunlop, J. S., Edge, A. C., Farrah, D., Geach, J. E., Hartley, W. G., Ivison, R. J., Karim, A., Lani, C., Ma, C. J., Meijerink, R., Michałowski, M. J., Mortlock, A., Scott, D., Simpson, C. J., Spaans, M., Thomson, A. P., van Kampen, E., & van der Werf, P. P. 2015, The SCUBA-2 Cosmology Legacy Survey: ALMA Resolves the Rest-frame Far-infrared Emission of Sub-millimeter Galaxies. *ApJ*, 799(1), 81.

Song, Y., Linden, S. T., Evans, A. S., Barcos-Muñoz, L., Murphy, E. J., Momjian, E., Díaz-Santos, T., Larson, K. L., Privon, G. C., Huang, X., Armus, L., Mazzarella, J. M., U, V., Inami, H., Charmandaris, V., Ricci, C., Emig, K. L., McKinney, J., Yoon, I., Kunneriath, D., Lai, T. S. Y., Rodas-Quito, E. E., Saravia, A., Gao, T., Meynardie, W., & Sanders, D. B. 2022, Characterizing Compact 15-33 GHz Radio Continuum Sources in Local U/LIRGs. *ApJ*, 940(1), 52.

Spilker, J. S., Marrone, D. P., Aravena, M., Béthermin, M., Bothwell, M. S., Carlstrom, J. E., Chapman, S. C., Crawford, T. M., de Breuck, C., Fassnacht, C. D., Gonzalez, A. H., Greve, T. R., Hezaveh, Y., Litke, K., Ma, J., Malkan, M., Rotermund, K. M., Strandet, M., Vieira, J. D., Weiss, A., & Welikala, N. 2016, ALMA Imaging and Gravitational Lens Models of South Pole Telescope – Selected Dusty, Star-Forming Galaxies at High Redshifts. *ApJ*, 826, 112.

Su, T., Marriage, T. A., Asboth, V., Baker, A. J., Bond, J. R., Crichton, D., Devlin, M. J., Dünner, R., Farrah, D., Frayer, D. T., Gralla, M. B., Hall, K., Halpern, M., Harris, A. I., Hilton, M., Hincks, A. D., Hughes, J. P., Niemack, M. D., Page, L. A., Partridge, B., Rivera, J., Scott, D., Sievers, J. L., Thornton, R. J., Viero, M. P., Wang, L., Wollack, E. J., & Zemcov, M. 2017, On the redshift distribution and physical properties of ACT-selected DSFGs. *MNRAS*, 464, 968–984.

Thompson, T. A., Quataert, E., & Murray, N. 2005, Radiation Pressure-supported Starburst Disks and Active Galactic Nucleus Fueling. *ApJ*, 630(1), 167–185.

Trombetti, T., Burigana, C., Bonato, M., Herranz, D., De Zotti, G., Negrello, M., Galluzzi, V., & Massardi, M. 2021, Search for candidate strongly lensed dusty galaxies in the Planck satellite catalogues. *A&A*, 653, A151.

Utomo, D., Sun, J., Leroy, A. K., Kruijssen, J. M. D., Schinnerer, E., Schruba, A., Bigiel, F., Blanc, G. A., Chevance, M., Emsellem, E., Herrera, C., Hygate, A. P. S., Kreckel, K., Ostriker, E. C., Pety, J., Querejeta, M., Rosolowsky, E., Sandstrom, K. M., & Usero, A. 2018, Star Formation Efficiency per Free-fall Time in nearby Galaxies. *ApJL*, 861(2), L18.

Vegetti, S., Koopmans, L. V. E., Auger, M. W., Treu, T., & Bolton, A. S. 2014, Inference of the cold dark matter substructure mass function at z = 0.2 using strong gravitational lenses. *MNRAS*, 442(3), 2017–2035.

Vegetti, S., Lagattuta, D. J., McKean, J. P., Auger, M. W., Fassnacht, C. D., & Koopmans, L. V. E. 2012, Gravitational detection of a low-mass dark satellite galaxy at cosmological distance. *Nature*, 481(7381), 341–343.

Vieira, J. D., Crawford, T. M., Switzer, E. R., Ade, P. A. R., Aird, K. A., Ashby, M. L. N., Benson, B. A., Bleem, L. E., Brodwin, M., Carlstrom, J. E., Chang, C. L., Cho, H. M., Crites, A. T., de Haan, T., Dobbs, M. A., Everett, W., George, E. M., Gladders, M., Hall, N. R., Halverson, N. W., High, F. W., Holder, G. P., Holzapfel, W. L., Hrubes, J. D., Joy, M., Keisler, R., Knox, L., Lee, A. T., Leitch, E. M., Lueker, M., Marrone, D. P., McIntyre, V., McMahon, J. J., Mehl, J., Meyer, S. S., Mohr, J. J., Montroy, T. E., Padin, S., Plagge, T., Pryke, C., Reichardt, C. L., Ruhl, J. E., Schaffer, K. K., Shaw, L., Shirokoff, E., Spieler, H. G., Stalder, B., Staniszewski, Z., Stark, A. A., Vanderlinde, K., Walsh, W.,

Williamson, R., Yang, Y., Zahn, O., & Zenteno, A. 2010, Extragalactic Millimeter-wave Sources in South Pole Telescope Survey Data: Source Counts, Catalog, and Statistics for an 87 Square-degree Field. *ApJ*, 719(1), 763–783.

Wardlow, J. L., Cooray, A., De Bernardis, F., Amblard, A., Arumugam, V., Aussel, H., Baker, A. J., Béthermin, M., Blundell, R., Bock, J., Boselli, A., Bridge, C., Buat, V., Burgarella, D., Bussmann, R. S., Cabrera-Lavers, A., Calanog, J., Carpenter, J. M., Casey, C. M., Castro-Rodríguez, N., Cava, A., Chanial, P., Chapin, E., Chapman, S. C., Clements, D. L., Conley, A., Cox, P., Dowell, C. D., Dye, S., Eales, S., Farrah, D., Ferrero, P., Franceschini, A., Frayer, D. T., Frazer, C., Fu, H., Gavazzi, R., Glenn, J., González Solares, E. A., Griffin, M., Gurwell, M. A., Harris, A. I., Hatziminaoglou, E., Hopwood, R., Hyde, A., Ibar, E., Ivison, R. J., Kim, S., Lagache, G., Levenson, L., Marchetti, L., Marsden, G., Martinez-Navajas, P., Negrello, M., Neri, R., Nguyen, H. T., O'Halloran, B., Oliver, S. J., Omont, A., Page, M. J., Panuzzo, P., Papageorgiou, A., Pearson, C. P., Pérez-Fournon, I., Pohlen, M., Riechers, D., Rigopoulou, D., Roseboom, I. G., Rowan-Robinson, M., Schulz, B., Scott, D., Scoville, N., Seymour, N., Shupe, D. L., Smith, A. J., Streblyanska, A., Strom, A., Symeonidis, M., Trichas, M., Vaccari, M., Vieira, J. D., Viero, M., Wang, L., Xu, C. K., Yan, L., & Zemcov, M. 2013, HerMES: Candidate Gravitationally Lensed Galaxies and Lensing Statistics at Submillimeter Wavelengths. *ApJ*, 762, 59.

Weiss, A., De Breuck, C., Marrone, D. P., Vieira, J. D., Aguirre, J. E., Aird, K. A., Aravena, M., Ashby, M. L. N., Bayliss, M., Benson, B. A., Béthermin, M., Biggs, A. D., Bleem, L. E., Bock, J. J., Bothwell, M., Bradford, C. M., Brodwin, M., Carlstrom, J. E., Chang, C. L., Chapman, S. C., Crawford, T. M., Crites, A. T., de Haan, T., Dobbs, M. A., Downes, T. P., Fassnacht, C. D., George, E. M., Gladders, M. D., Gonzalez, A. H., Greve, T. R., Halverson, N. W., Hezaveh, Y. D., High, F. W., Holder, G. P., Holzapfel, W. L., Hoover, S., Hrubes, J. D., Husband, K., Keisler, R., Lee, A. T., Leitch, E. M., Lueker, M., Luong-Van, D., Malkan, M., McIntyre, V., McMahon, J. J., Mehl, J., Menten, K. M., Meyer, S. S., Murphy, E. J., Padin, S., Plagge, T., Reichardt, C. L., Rest, A., Rosenman, M., Ruel, J., Ruhl, J. E., Schaffer, K. K., Shirokoff, E., Spilker, J. S., Stalder, B., Staniszewski, Z., Stark, A. A., Story, K., Vanderlinde, K., Welikala, N., & Williamson, R. 2013, ALMA Redshifts of Millimeter-selected Galaxies from the SPT Survey: The Redshift Distribution of Dusty Star-forming Galaxies. *ApJ*, 767, 88.

Wilson, G. W., Abi-Saad, S., Ade, P., Aretxaga, I., Austermann, J., Ban, Y., Bardin, J., Beall, J., Berthoud, M., Bryan, S., Bussan, J., Castillo, E., Chavez, M., Contente, R., DeNigris, N. S., Dober, B., Eiben, M., Ferrusca, D., Fissel, L., Gao, J., Golec, J. E., Golina, R., Gomez, A., Gordon, S., Gutermuth, R., Hilton, G., Hosseini, M., Hubmayr, J., Hughes, D., Kuczarski, S., Lee, D., Lunde, E., Ma, Z., Mani, H., Mauskopf, P., McCrackan, M., McKenney, C., McMahon, J., Novak, G., Pisano, G., Pope, A., Ralston, A., Rodriguez, I., Sánchez-Argüelles, D., Schloerb, F. P., Simon, S., Sinclair, A., Souccar, K., Torres Campos, A., Tucker, C., Ullom, J., Van Camp, E., Van Lanen, J., Velazquez, M., Vissers, M., Weeks, E., & Yun, M. S. The TolTEC camera: an overview of the instrument and in-lab testing results. In Zmuidzinas, J. & Gao, J.-R., editors, *Millimeter, Submillimeter, and Far-Infrared Detectors and Instrumentation for Astronomy X* 2020, volume 11453 of *Society of Photo-Optical Instrumentation Engineers (SPIE) Conference Series*, 1145302.